Journal of Statistical Physics, Vol. 78, Nos. 5/6, 1995

Phase Transitions in a Driven Lattice Gas in Two Planes

A. Achahbar[1] **and J. Marro**[1]

Received October 18, 1993; final September 6, 1994

We report on a Monte Carlo study of ordering in a nonequilibrium system. The system is a lattice gas that comprises two equal, parallel square lattices with stochastic particle-conserving irreversible dynamics. The particles are driven along a principal direction under the competition of the heat bath and a large, constant external electric field. There is attraction only between particles on nearest-neighbor sites within the same lattice. Particles may jump from one plane to the other; therefore, density fluctuations have an extra mechanism to decay and build up. It helps to obtain the steady-state accurately. Spatial correlations decay with distance according to a power law at high enough temperature, as for the ordinary two-dimensional case. We find two kinds of nonequilibrium phase transitions. The first one has a critical point for half occupation of the lattice, and seems to be related to the anisotropic phase transition reported before for the plane. This transition becomes discontinuous for low enough density. The difference of density between the planes changes discontinuously for any density at a lower temperature. This seems to correspond to a phase transition that does not have a counterpart in equilibrium nor in the two-dimensional nonequilibrium case.

KEY WORDS: Driven lattice gas; steady nonequilibrium states; nonequilibrium phase transitions; nonequilibrium critical behavior; Monte Carlo simulation.

1. INTRODUCTION

Quantitative studies by the Monte Carlo (MC) method of phase transitions in lattice gases with particle-conserving dynamics are difficult. In practice, a large, often prohibitive amount of computer time is required to obtain reliable results. The reason is that, besides critical slowing down, a

[1] Instituto Carlos I de Física Teórica y Computacional, and Departamento de Física Aplicada, Facultad de Ciencias, Universidad de Granada, E-18071-Granada, Spain.

0022-4715/95/0300-1493$07.50/0

system exhibits slow relaxation toward ordered steady states if the only mechanism is (e.g.) nearest-neighbor exchanges, i.e., diffusion of particles. It has been reported for the *driven lattice gas* system[1,2] (DLG), for example, which models certain features of solid electrolytes.[3] Previous numerical work[4-9,2] has revealed that one may obtain statistically good enough stationary mean values for short-ranged order parameters and electrical currents, for instance, while (e.g.) the structure function stabilizes very rarely if at all within actual computer runs. Thus, much of the interesting behavior of the DLG as one varies its parameters is known within approximations, namely mean-field treatments of the lattice system[1] and field-theoretic studies of related continuum models.[10-13] As a consequence of the intrinsic difficulties in obtaining good data for the DLG (where anisotropies, slow spatial decay of correlations,..., and lack of nonequilibrium theory add up to slow diffusive relaxation under a conserved density), a controversy exists concerning critical behavior.[10] That is, MC data for the two-dimensional DLG under a saturating field (2d DLG hereafter) seems to indicate that the critical exponent for the order parameter is $\beta \approx 1/4$,[7] while field theory suggests that $\beta = 1/2$ *subject to possible logarithmic corrections.*[10]

We report in this paper on the results from an extensive MC study of a variation of the 2d DLG. Our model incorporates an additional degree of freedom, i.e., the particles can hop to other lattice. As a consequence, (slow) diffusion within the plane is not the only mechanism that allows for relaxation. This occurs also at equilibrium, i.e., when *the field is turned off*, in which case a simple relation may be stated rigorously between the behavior of such modification and the ordinary 2d case.[14] The relation is conceptually less simple out of equilibrium. This interesting case that involves the effects of both an external force and a conserved density on layered systems is studied in detail below. It may have some relevance for *quasi-two-dimensional* conduction that has been reported (e.g.) for some solid electrolytes[1,3] in which ions are compelled to move within a plane geometry that comprises a few layers only. We have also addressed the relation between the steady states for this system and for the ordinary 2d DLG. It has led us to some interesting conclusions about critical behavior in nonequilibrium phase transitions in anisotropic systems.

The basic model is defined in Section 2, which contains also a description of a few general properties of the model and some details of its MC

[2] The standard DLG is modified in ref. 9 by adding a small amount of creation–annihilation to the original diffusion process to speed up the relaxation in the computer.

implementation. Some main results from our MC study are reported in Section 3. Section 4 contains a brief discussion.

2. THE MODEL SYSTEM

Let us denote by λ the ordinary lattice gas[15] on a finite square lattice of *volume* $|\lambda|$ with periodic boundary conditions. The configurational energy is

$$H(\sigma) = -4J \sum_{|\mathbf{r}-\mathbf{s}|=1} \sigma_{\mathbf{r}}\sigma_{\mathbf{s}}, \qquad J>0 \tag{2.1}$$

where $\sigma = \{\sigma_{\mathbf{r}};\ \mathbf{r}\in\mathbf{Z}^2,\ \sigma_{\mathbf{r}}=0,1\}$, and the sum is over all pairs $(\mathbf{r},\mathbf{s})$ of nearest neighbor (NN) lattice sites. Thus, $\rho \equiv |\lambda|^{-1}\sum_{\mathbf{r}}\sigma_{\mathbf{r}}$ is a density, and $N \equiv \rho\,|\lambda|$ is the number of *particles* (i.e., states $\sigma_{\mathbf{r}}=1$); the sites for which $\sigma_{\mathbf{r}}=0$ are *empty*. In the infinite-volume limit, λ is known to exhibit a critical point for $\rho = 1/2$ at the *Onsager temperature* T_C (we use $T_C = 2.269J/k_B$ as a unit for temperature throughout), and a coexistence line occurs for $\rho \neq 1/2$ at temperature $T_{LG}(\rho)$; cf. Table I.

Next, consider the system $\Lambda \equiv \lambda_1 \cup \lambda_2$ of volume $|\Lambda| = 2\,|\lambda|$; here both λ_1 and λ_2 are defined like λ, and $\lambda_1 \cap \lambda_2 = \varnothing$. That is, Λ consists of two twin square lattices such that any site has five NN with one of them in the other plane. The configurations of Λ have energy

$$H_\Lambda(\sigma) = H(\sigma^1) + H(\sigma^2) \tag{2.2}$$

Table I. Variation with Density of the Transition Temperature for Several Systems in Units of the Onsager Critical Temperature T_C[a]

System	λ	Λ	λ_∞	Λ_∞	Λ_∞
ρ	T_{LG}	T^*	T_∞	T^*_∞	T'_∞
0.50	1	1	1.38	1.30	0.95
0.35	0.99999	~ 1	1.30	1.24	0.89
0.20	0.997	0.97	1.16	1.14	0.88
0.10	0.964	0.93	0.84	0.93	0.85

[a] T_{LG} is for the ordinary 2d lattice gas, λ; thus, $T_{LG}(\rho = 1/2) = T_C$ by definition. T^* is the MC estimate for the quasi-2d equilibrium system Λ.[14] T_∞ is for the 2d DLG as reported here and in ref. 8. T'_∞ is for the onset of the anisotropic, striplike segregation of the liquid in one of the planes only, as observed for the nonequilibrium system Λ_∞ at low enough temperatures. T^*_∞ is for the formation of strips within the two planes of Λ_∞ at a relatively higher temperature. Error bars for Λ_∞ are typically smaller than 0.02 for $\rho = 1/2$ and at least 0.05 for $\rho = 0.1$; cf. Section 4.

where $\sigma^i = \{\sigma_{\mathbf{r}}; \mathbf{r} \in \mathbf{Z}^2\}$ represents a configuration of λ_i, and $i = 1, 2$. Consequently, any two particles interact with each other [in fact, they attract given the restriction to $J > 0$ in (2.1)] only if they are at NN sites such that both belong either to λ_1 or to λ_2; i.e., all bonds between the planes are broken. No restriction exists on the possible configurations $\boldsymbol{\sigma}$ of Λ, however; in particular, any given particle has access to any of the two sublattices.

Irreversibility is introduced into the problem by considering the following Markovian time evolution. The probability of any configuration at time t, to be denoted $P_E(\boldsymbol{\sigma}; t)$, is governed by the master equation[1,2]

$$\partial P_E(\boldsymbol{\sigma}; t)/\partial t = \sum_{\boldsymbol{\sigma}^{\mathbf{rs}}} [c_E(\boldsymbol{\sigma}^{\mathbf{rs}}; \mathbf{r}, \mathbf{s}) P_E(\boldsymbol{\sigma}^{\mathbf{rs}}; t) - c_E(\boldsymbol{\sigma}; \mathbf{r}, \mathbf{s}) P_E(\boldsymbol{\sigma}; t)] \tag{2.3}$$

Here, $\boldsymbol{\sigma}^{\mathbf{rs}}$ represents $\boldsymbol{\sigma}$ with the occupation variables at NN sites $\mathbf{r}$ and $\mathbf{s}$ exchanged, and $c_E(\boldsymbol{\sigma}; \mathbf{r}, \mathbf{s})$ is the transition probability per unit time for that exchange, given $\boldsymbol{\sigma}$. Consequently, time evolution proceeds by stochastic jumps of particles to NN empty sites that includes jumps from one plane to the other. The jumps are driven by the competition between a heat bath at temperature T and an external *electric* field $\mathbf{E}$. The latter is constant in both space and time; it points along one of the principal lattice directions. Such a process may be simulated by choosing the transition probability in (2.3) as

$$c_E(\boldsymbol{\sigma}; \mathbf{r}, \mathbf{s}) = f[\beta H_\Lambda(\boldsymbol{\sigma}^{\mathbf{rs}}) - \beta H_\Lambda(\boldsymbol{\sigma}) - \mathbf{E} \cdot (\mathbf{r} - \mathbf{s})(\sigma_{\mathbf{r}} - \sigma_{\mathbf{s}})] \tag{2.4}$$

where $\beta = (k_B T)^{-1}$ is the inverse temperature, and $|\mathbf{r} - \mathbf{s}| = 1$. The function $f(X)$ is arbitrary except that $f(X) = e^{-X} f(-X)$, which guaranties that $c_E(\boldsymbol{\sigma}; \mathbf{r}, \mathbf{s})$ satisfies the familiar condition of detailed balance for $E = 0$ [it is convenient to require also $f(0) = 1$, and $f(X) \to 0$ as $X \to \infty$]. Thus, (2.3)–(2.4) imply an asymptotic tendency toward canonical equilibrium for $E = 0$. For $E \neq 0$, $c_E(\boldsymbol{\sigma}; \mathbf{r}, \mathbf{s})$ introduces a preferential hopping in the field direction that impedes detailed balance except locally; more explicitly, the electric energy cannot be added to the configurational energy in the Hamiltonian, but the work done by the field has been included in (2.4), which induces a net steady dissipative current (e.g.) for periodic boundary conditions (cf. ref. 2 for further discussion and for an alternative way to induce the current). Let us denote by λ_E and Λ_E the nonequilibrium systems one obtains from λ and Λ, respectively, under dynamics (2.3)–(2.4); λ_E corresponds to the 2d DLG; Λ_E is the specific system of interest here.

The (equilibrium) phase diagram for Λ (i.e., Λ_E when the field is turned off) is interesting[14]: For $\rho = 1/2$ below a temperature T^*, a *liquid*

phase of density $\rho_L(T)=\rho_0(T)$ fills one of the planes and a *gas* of density $\rho_G(T)=1-\rho_0(T)$ fills the other plane; $\rho_0(T)$ is the Onsager solution, i.e.,

$$\rho_0(T)=1/2+1/2\{1-[\sinh(2J/k_B T)]^{-4}\}^{1/8}, \qquad T<T^*(\rho=1/2) \tag{2.5}$$

For $\rho<1/2$ below $T^*(\rho)$, one plane holds a *liquid drop* of density $\rho_0(T)$ coexisting with gas of density $1-\rho_0(T)$, and there is only gas in the other plane. Once the number of particles is given, the fraction x of liquid phase is smaller for Λ than for λ: some particles need to go to the other plane. That is, $\rho=1/2\rho_G+1/2[x\rho_L+(1-x)\rho_G]$, and there follows $x=2(\rho-1+\rho_0)/(2\rho_0-1)$. The particles tend to be distributed homogeneously for $T>T^*(\rho)$, where the latter is given by $\rho=1-\rho_0(T^*)$; thus, $T^*(\rho)=T_{LG}(\rho)$ (the transition temperature for λ); in particular, $T^*(\rho=1/2)=T_C$ (cf. Table I). Therefore, it is natural to look at a (nonconserved) order parameter defined as the difference of density between the two planes,

$$\Delta\rho(T)\equiv(1/2\rho)\,|\rho_1(T)-\rho_2(T)| \tag{2.6}$$

Then, $\Delta\rho(T)=\rho^{-1}\,|\rho-1+\rho_0(T)|$. This is continuous for any ρ and, in particular, it implies that Λ has the Onsager critical point for $\rho=1/2$.

We are interested in the present paper in the nature of the steady states for Λ_∞, which denotes Λ_E within the limit $E\to\infty$. Some specific questions of interest are the influence on thermodynamics of the extra degree of freedom in Λ, the nature of the expected phase transitions in Λ_∞, and their relation to the ones in λ_∞ (the 2d DLG).

Some details of our computer implementation of Λ_∞ are as follows. One chooses an arbitrary initial configuration. In practice, we have used either a completely random one simulating a very high-temperature state with no field, or else an ordered one, e.g., all the particles arbitrarily clustered in only one plane (or as obtained in a previous experiment at a different temperature). Then, one performs the following *MC step* reiteratively: One selects at random a particle $\sigma_r=1$ and one of its NN holes, $\sigma_s=0$, and one attempts the interchange $\sigma_r\rightleftarrows\sigma_s$. It is performed (rejected) if it implies a jump of the particle in (against) the direction of the field, which aims to simulate the case of an infinite or saturating field, $E=\infty$. For attempted jumps perpendicular to the field, including jumps to the other lattice, one computes $\Delta H\equiv H_\Lambda(\sigma^{rs})-H_\Lambda(\sigma)$ [which does not involve any interaction between planes; cf. Eq. (2.2)] and uses the Metropolis algorithm, namely, the jump is performed with probability $p=\min\{1,\exp(-\beta\,\Delta H)\}$. The initial time evolution obtained in this way is discarded until the system reaches the stationary regime; this is decided by eventual statistical analysis of fluctuations and of the structure function.

The system sizes investigated in practice have ranged from $|\Lambda| = 2 \times 4 \times 4$ to $2 \times 140 \times 140$ (eventually, we also considered some rectangular geometries, i.e., $2 \times L_v \times L_h$ lattices). More than 10^6 MC steps (per lattice site) have been performed within the stationary regime to obtain good statistics for large $|\Lambda|$. Typical error bars are smaller than the size of the symbols used in the graphs, unless otherwise indicated.

3. ANALYSIS OF COMPUTER RESULTS

Direct inspection of MC configurations suggests the following picture. At high enough T, the particles distribute evenly between the two planes of Λ_∞. The distribution within each plane is not completely homogeneous, but some anisotropic clustering is evident (cf. Figs. 1a and 1d, for instance). This was first reported for the 2d DLG[6,7]; it reflects the anisotropy of the state, and perhaps also the slow decay of spatial correlations that seems to characterize the high-temperature phase; it is analyzed below. As T is lowered starting from a random distribution, the system exhibits phase segregation and apparently two kinds of transitions:

(a) For very low temperature, say $T < T'_\infty(\rho)$, the particle-rich or *liquid* phase is in one plane, as illustrated in Figs. 1c and 1f. This is qualitatively similar to the segregation that occurs in λ_∞ except for the existence of the second plane holding the gas. The field induces clear anisotropies below $T'_\infty(\rho)$. That is, the liquid configurations are striplike oriented parallel to the field for $\rho < 1/2$, as for λ_∞.[7,8] Moreover, the gas seems to exhibit the sort of anisotropic clustering that we mentioned above for high T; see below.

(b) For not so low temperature, say $T^*_\infty(\rho) > T > T'_\infty(\rho)$, one observes that the liquid separates into two approximately equal strips, *one on top of the other* in a different plane; this is illustrated in Figs. 1b and 1e. We remark that segregation in two planes has been reported to correspond for Λ to a sort of (rare, i.e., segregated) metastability[14]; this is not so for Λ_∞, however, where it seems to correspond to the only stable states within the indicated temperature range due to the existence of a current between planes along the interfaces.

The relation between Λ and Λ_∞ is not straightforward. A main effect of the field is to modify the interface (and, apparently, the correlations also; see below), so that the density of the liquid, which is $\rho_0(T)$ at equilibrium, changes to $\rho_\infty(T)$. That is, $\rho_\infty(T) \neq \rho_0(T)$, which makes the liquid fraction x and, consequently, the transition temperature differ from the ones for the equilibrium case. For simplicity, however, one may expect that Λ_∞ and λ_∞ exhibit the same (second-order) phase transition, as is known to occur at

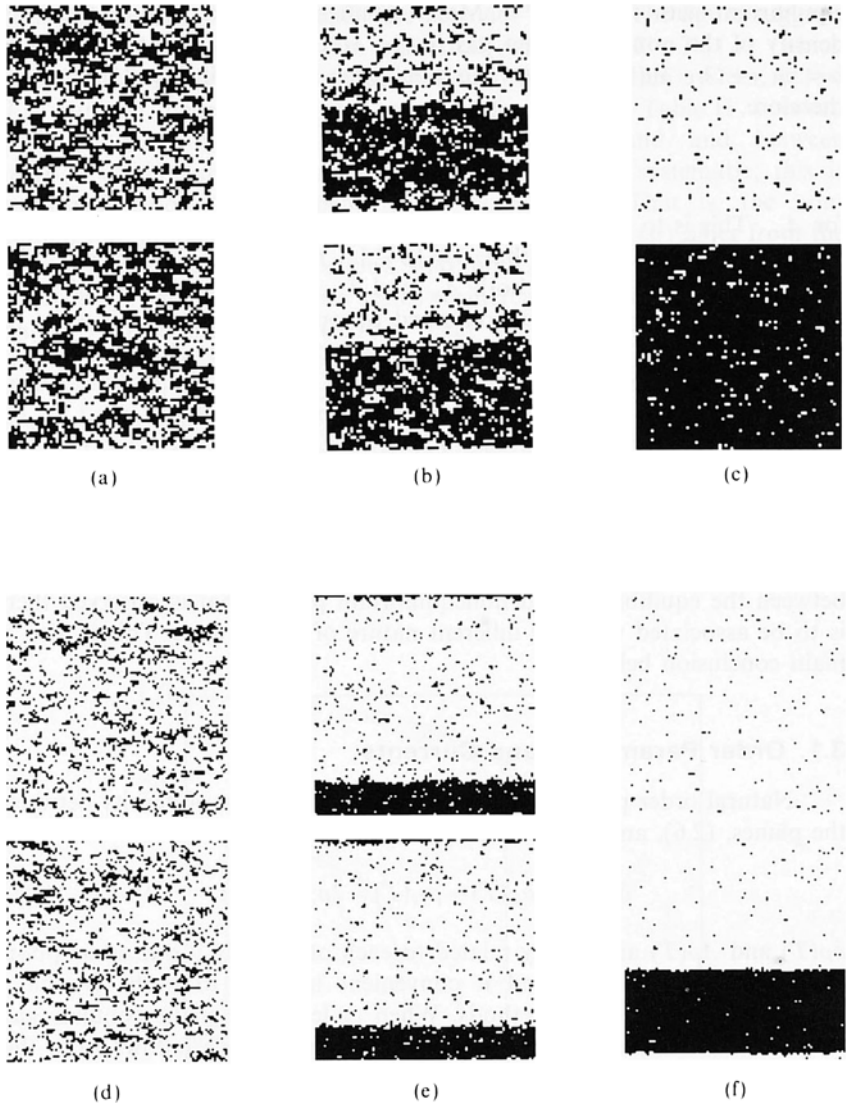

Fig. 1. Some typical steady-state configurations for the two planes of Λ_x; the field acts horizontally. (a) In the one-phase region for $\rho = 1/2$ at $T = 1.39T_C > T_x^*(\rho)$. (b) Same system within the *intermediate region*, namely at $T = 1.22T_C < T_x^*(\rho = 1/2)$, which is above $T'_x(\rho = 1/2)$. (c) Same system at $T = 0.90T_C < T'_x(\rho = 1/2)$. (d) In the one-phase region for $\rho = 0.20$ at $T = 1.15T_C > T_x^*(\rho)$. (e) Same system ($\rho = 0.2$) within the *intermediate region*, namely at $T = 0.90T_C < T_x^*(\rho)$, which is above $T'_x(\rho)$. (f) Same system at $T = 0.70T_C < T'_x(\rho)$.

equilibrium with λ and Λ.[14] More specifically, let us assume that the density of the nonequilibrium gas in Λ_∞ is $1-\rho_\infty(T)$, and that one has $\rho = x\rho_\infty + (1-x)(1-\rho_\infty)$ for situations such as those in Figs. 1b and 1e; therefore,

$$x = (\rho - 1 + \rho_\infty)/(2\rho_\infty - 1) \tag{3.1}$$

for Λ_∞. This is to be compared with $x = 2(\rho - 1 + \rho_0)/(2\rho_0 - 1)$ for Λ. We would expect accordingly that $x = (\rho - 1 + \rho'_\infty)/(2\rho'_\infty - 1)$ for λ_∞. The simplest assumption is that both Λ_∞ and λ_∞ have the same critical point for $\rho = 1/2$. It seems roughly confirmed by our analysis below in spite of the fact that we have observed a different temperature for Λ_∞ than for λ_∞. For $\rho < 1/2$, the condensed plane of Λ_∞ for $T < T'_\infty(\rho)$ would be identical to λ_∞ if $\rho'_\infty(T) = \rho_\infty(T)$; otherwise, the respective densities need to be related as $\rho_\Lambda[2\rho'_\infty(T) - 1] - \rho'_\infty(T) = \rho_\lambda[2\rho_\infty(T) - 1] - \rho_\infty(T)$. On the other hand, the difference between $\rho_\infty(T)$ and $\rho_0(T)$ is large when configurations are striped due to the presence of the nonequilibrium interface all along the system. When no interface exists the difference between $\rho_\infty(T)$ and $\rho_0(T)$ is extremely small in general; the small difference between the equilibrium and nonequilibrium phases that is observed then is to be associated with the different nature of correlations. This is also a main conclusion below.

3.1. Order Parameters and Currents

Natural order parameters for Λ_∞ are the difference of density between the planes, (2.6), and between the phases,

$$\delta\rho(T) \equiv \rho_L(T) - \rho_G(T) = 2\rho_\infty(T) - 1 \tag{3.2}$$

$\delta\rho(T)$ and $\Delta\rho(T)$ are closely related to each other only if our assumption (3.1) holds, so that we find it convenient to refer to both. We have estimated $\rho_\infty(T)$ by two methods. When at least one plane contains gas only, a good estimate for the density of the gas $\rho_G(T)$ follows from the number of particles in that plane. Then, the fraction of liquid in the other plane may be estimated as $x = \sum_i l_i/|\Lambda|$, where l_i ($i = 1, 2, \ldots, L$) is the local width of the strip, and one has that $\rho_\infty(T) = \rho_L(T) = 2[\rho - \rho_G(T)]/x + \rho_G(T)$. Our estimate is less accurate if both planes contain segregation; e.g., it occurs at high temperature, where it is difficult in practice to figure out the precise spatial extension of each phase due, in particular, to roughness of the interface. Anyhow, the data then confirm that $\rho_L + \rho_G = 1$ within less than 1% error for any ρ and T. On the other

hand, Fig. 2 and Table II depict the behavior of (3.2). The figure suggests that $\rho_\infty(T, \rho) = \rho_0(T, \rho)$ within statistical errors for $T < T'_\infty(\rho)$ (which would imply a very simple picture for the nonequilibrium system at low T), but we believe that the small differences in Table II between $\rho_\infty(T, \rho = 1/2)$ and $\rho_0(T, \rho = 1/2)$ on the one hand and between $\rho_\infty(T, \rho = 1/2)$ and $\rho_\infty(T, \rho = 0.35)$ on the other are systematic; this is confirmed below by the behavior of correlations. That is, the nonequilibrium liquid and gas phases for $\rho = 1/2$ at $T < T'_\infty(\rho)$ differ from the equilibrium ones. Table II shows that $\delta\rho(T, \rho = 1/2)$ is larger in nonequilibrium, and the difference seems to increase with T (while we do not find any difference for $T \leqslant 0.6 T_C$). What is clearly observed in Fig. 2 is that $\delta\rho(T, \rho)$ $[= 2\rho_\infty(T, \rho) - 1]$ is discontinuous at $T = T^*_\infty(\rho)$ for $\rho \ll 1/2$; it also seems to be discontinuous at $T = T'_\infty(\rho)$ for any ρ, namely, $\delta\rho(T)$ apparently increases when one crosses $T'_\infty(\rho)$ for any ρ as T is increased. The latter fact probably reflects a similar discontinuous behavior of the interface. One also observes an apparent tendency of $\delta\rho(T)$ to decrease with decreasing ρ for a given $T < T'_\infty(\rho)$ (cf. Table II). These facts are confirmed by $\Delta\rho(T, \rho)$ when possible; anyhow, our error bars are relatively large for $\rho < 1/2$.

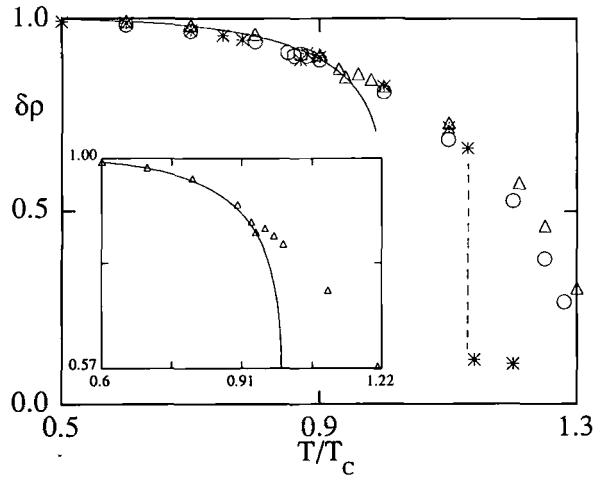

Fig. 2. The difference of density between the phases, (3.2), as a function of T for representative values of ρ: $\rho = 0.5$ (triangles), 0.35 (circles), and 0.2 (asterisks). (Some of the values plotted here are reported in Table II.) The solid line is the Onsager result; the dashed line is a guide to the eye. The inset shows the case $\rho = 1/2$ in more detail. Typical error bars here are of the order of the symbol sizes.

Table II. MC Estimates for the Parameter (3.2) for Representative Values of T for $\rho = 1/2$ and 0.35[a]

	Onsager	Nonequilibrium	
T/T_C	$\rho = 1/2$	$\rho = 1/2$	$\rho = 0.35$
0.6	0.993	0.993	0.984
0.7	0.981	0.982	0.967
0.8	0.955	0.959	0.940
0.9	0.895	0.906	0.893
0.93	0.863	0.870	—
0.98	0.748	0.842	—

[a] The table reveals systematic differences that are not obvious on the scale of Fig. 2 (cf. Fig. 10 for a graphic, independent confirmation of such a difference for $T = 0.8T_C$ and $\rho = 1/2$). The Onsager result (for $E = 0$) is also shown.

We have found it convenient to monitor the underlying anisotropy by measuring at each plane, $i = 1, 2$, the parameter[4]

$$m_i = 1/2[\rho(1-\rho)]^{-1/2} \, |\langle \mathbf{M}_h^2 \rangle - \langle \mathbf{M}_v^2 \rangle|^{1/2} \tag{3.3a}$$

where

$$\mathbf{M}_{h(v)}^2 = |\lambda|^{-3/2} \sum_{h(v)} \left[\sum_{v(h)} (1 - 2\sigma_r) \right]^2 \tag{3.3b}$$

Then, we define the maximum

$$m \equiv \max\{m_1, m_2\} \tag{3.3c}$$

Here, h (v) indicates that summation is along the horizontal (vertical) direction on each plane; we define the horizontal direction as the one along which the external field is directed. The behavior of m and $\Delta\rho(T)$, as defined in (2.6), is depicted in Fig. 3. This confirms that the phase transition at $T'_\infty(\rho)$ is discontinuous for any ρ, while the one at the higher temperature $T^*_\infty(\rho)$ is discontinuous for $\rho \ll 1/2$, but the discontinuities are very small, if any, as one approaches $\rho = 1/2$, and $T^*_\infty(\rho = 1/2)$ should correspond to a critical point for the infinite system. The phase diagram is sketched in Fig. 4, and the values for $T'_\infty(\rho)$ and $T^*_\infty(\rho)$ are reported in Table I. It is interesting to remark that the transition at $T^*_\infty(\rho)$ is the one to be compared to the transition at $T_\infty(\rho)$ for λ_∞. We believe that our values for $T^*_\infty(\rho)$ in Table I are more reliable as ρ is increased, and that they are rather good estimates for $\rho \geqslant 0.35$.

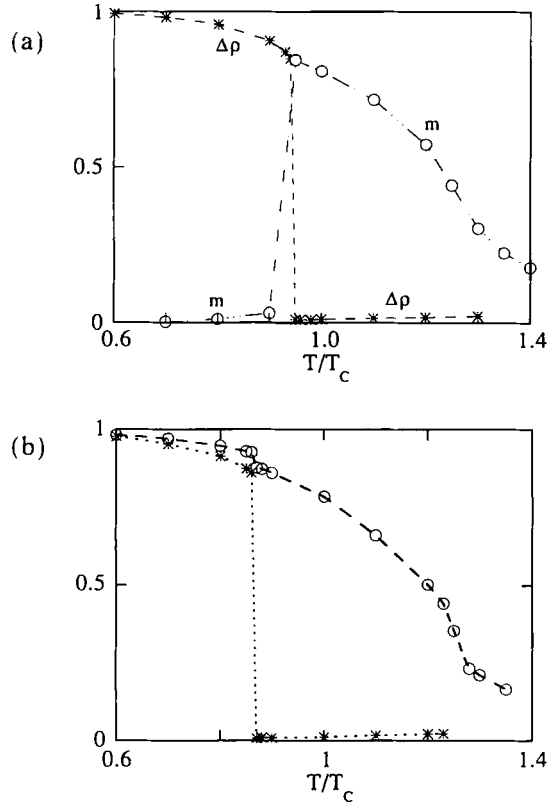

Fig. 3. The variation with temperature of the order parameters m (circles) and $\Delta\rho$ (asterisks), as given, respectively, by (3.3) and (2.6), for $\rho = 1/2$ (a), 0.35 (b), 0.2 (c), and 0.1 (d). The indicated transitions as one increases temperature are between states with one strip, with two strips, one at each plane, and with no strips, respectively.

In fact, we have generated data of very good quality for $\rho = 1/2$ to study critical behavior. Figure 5 illustrates $m(T)$ for several system sizes and the corresponding extrapolation for the infinite lattice, $|\Lambda| \to \infty$. No definite support was found for elaborate scaling formulas in the literature (see below); therefore, our extrapolation is the simplest one based on the apparent fact that the nonequilibrium interface induces strong surface effects that are *qualitatively* similar to the ones for the Ising model with free ends.[7] The comparison in the figure between $m(T)$ and the Onsager solution depicts a departure of the former from the equilibrium case (which is also quite evident near the critical temperature; a similar depar-

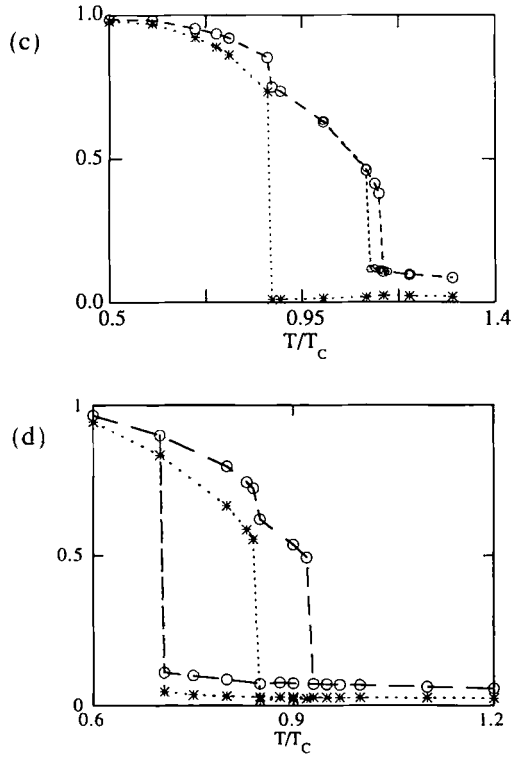

Fig. 3. (*Continued*)

ture occurs from other predictions). Further analysis of the data for the infinite lattice under the assumption

$$m \sim |T - T^*_\infty(\rho = 1/2)|^\beta \qquad \text{as} \quad T \to T^*_\infty(\rho = 1/2) \tag{3.4}$$

shows that β is close to 0.27. On the contrary, the Onsager case $\beta = 1/8$ is excluded [nor do the data admit $\beta = 1/2$ in (3.4) even if one allows for a (weak) logarithmic correction]. Figure 6 contains some evidence of these facts, which are confirmed by independent analysis below. It suggests again the crucial effect of the field due to the existence of a nonequilibrium interface. Our best estimates for the infinite lattice are $T^*_\infty(\rho = 1/2) = 1.30 \pm 0.01$ and $\beta = 0.27 \pm 0.02$ (the critical amplitude follows as $B = 1.25 \pm 0.03$). Furthermore, we have verified that $\Delta\rho(T)$ and $\delta\rho(T)$ have a similar critical behavior near $T^*_\infty(\rho = 1/2)$, as expected [the same method clearly indicates that $\delta\rho$ is characterized by $\beta \approx 1/8$ for $E = 0$, as predicted by (2.5);

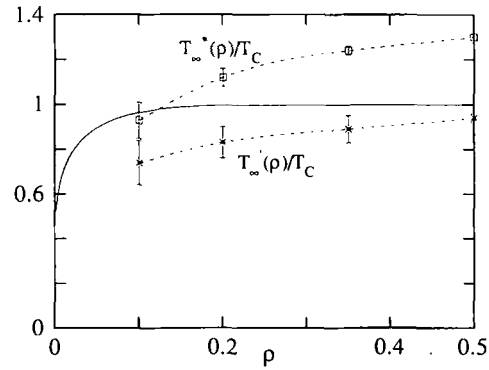

Fig. 4. The phase diagram indicating $T^*_\infty(\rho)$ and $T'_\infty(\rho)$; cf. Table I. The bars may be interpreted, approximately, as the observed limits of metastability. The solid line corresponds to the Onsager solution; the dashed lines are guides to the eye.

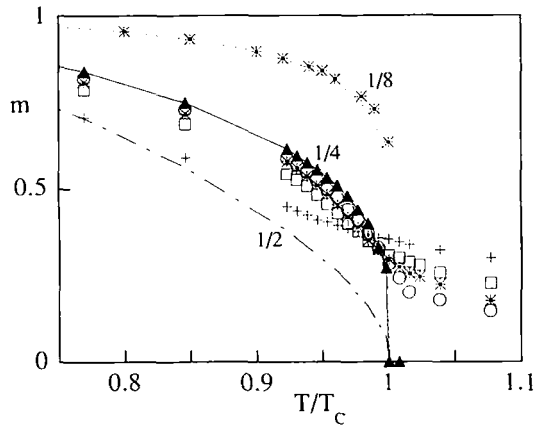

Fig. 5. The temperature variation of the parameter m in (3.3) for $\rho = 1/2$ and lattice sizes $L = 16$ (crosses), 32 (squares), 64 (asterisks), and 128 (circles). The solid line is a fit to the extrapolated values for $|A| \to \infty$ (solid triangles) giving approximately 1/4 near the critical temperature. The Onsager solution (dashed line, corresponding to 1/8) and corresponding MC results for $L = 128$ (asterisks) are indicated for comparison purposes; we have also indicated the mean-field result producing $\beta = 1/2$. The data are normalized to the corresponding critical temperature for each model (but no shift or scaling has been performed within the vertical axis).

cf. Fig. 5]. According to the assumed relation between Λ_∞ and λ_∞ (and our claim about the good quality of the data for $\rho = 1/2$), this value for β should perhaps replace the one in ref. 7 for the 2d DLG. The fact that $\beta \approx 1/4$ for Λ_∞ and for λ_∞ is in agreement with previous MC experiments, which suggested values of β close to 1/4 for several other nonequilibrium, 2d DLG-related conservative lattice systems that involve anisotropies.[9, 16–19] (Approximately the same value has been reported for a 2d field-theoretic driven system when the applied field is random,[20] but not for the present case of constant field.[10] Furthermore, the MC study of a lattice model of a fluid under shear gives some indications that $1/2 > \beta > 1/8$.[21] Thus, one may argue that a *universality class* exists corresponding to nonequilibrium systems such as the ones defined here and in refs. 7, 9, and 16–21. Anyhow, there is strong numerical evidence supporting $1/2 > \beta > 1/8$ for nonequilibrium lattice gases, which requires a theoretical explanation. It would also be interesting to look experimentally at critical behavior in materials under nonequilibrium anisotropic conditions.

Further quantities of interest are the currents, energy, and "specific heats." The particle current in the direction of the field, say j_x, is propor-

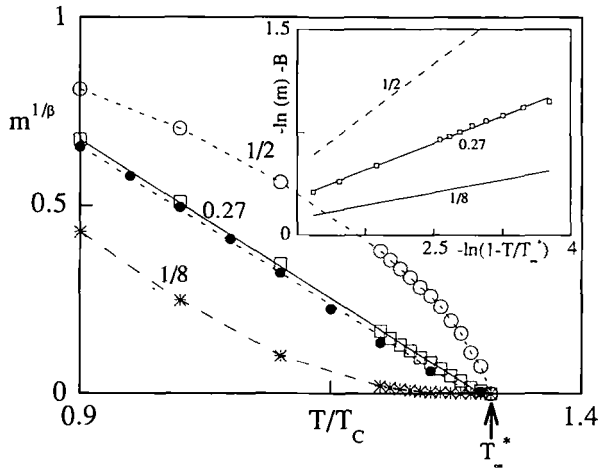

Fig. 6. Some evidence of a critical behavior of $m(T)$ for the infinite system that is characterized by an exponent $\beta \approx 1/4$, as explained in the text. The inset shows a log–log plot of the data assuming $T_\infty^* = 1.3$; this gives $\beta = 0.27$; the lines of slope 1/8 and 1/2 are also shown. The main graph shows plots of $m^{1/\beta}$ for different values of β (as indicated) versus T that avoids any assumption about T_∞^*; this gives a straight line only for β very close to 0.27. The solid circles correspond to the data for $n^{1/\beta}$ [cf. Eq. (3.7)] to show consistency of other order parameters with $\beta \approx 0.27$ also.

tional for large field to the density of particle–hole pairs averaged over the planes, say e; according to (2.1)–(2.2), the latter is a measure of the system energy.[7] The behavior of e and j_x is illustrated in Fig. 7. This reveals again the existence of the two mentioned phase transitions for each ρ. It is evident from the temperature derivative of e, say $\partial e/\partial T$. For $\rho = 1/2$, this derivative exhibits two pronounced peaks at T'_∞ and T^*_∞, respectively; the latter is such that no logarithmic divergence but $\alpha > 0$ seems suggested; our data are not enough to conclude about this matter, however. We have studied also the mean square fluctuations corresponding to the mean e, say δe. No evidence of a fluctuation-dissipation theorem for the 2d DLG was reported earlier[7]; we have observed, however, that δe and $\partial e/\partial T$ seem to tend to exhibit the same structure near T^*_∞ as $|\Lambda|$ is increased [while $\delta e(T)$ shows no evidence of such structure for $L \leqslant 64$, which may explain the reported observation[7] for the 2d DLG]. This is interesting because the continuum model that has been compared[10] to the DLG seems based on the breakdown of a fluctuation-dissipation relation; such a behavior is also not contained in a DLG model worked out analytically earlier.[1]

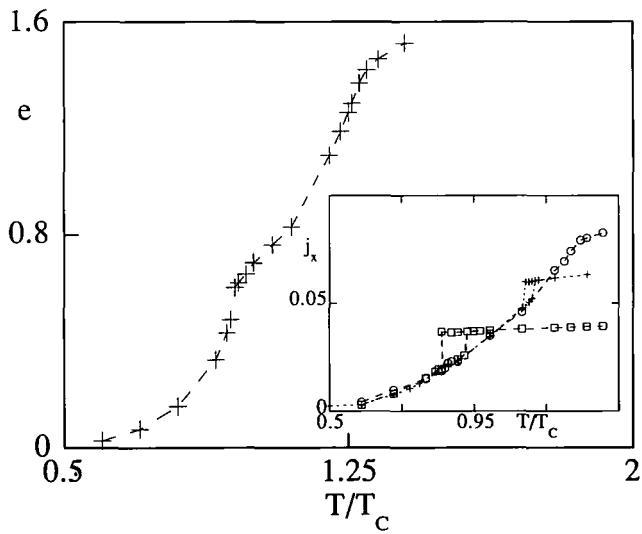

Fig. 7. The *energy* (density of particle–hole bonds averaged over the two planes) versus temperature for a finite lattice with $\rho = 1/2$. The two phase transitions are revealed by the two abrupt changes of slope that are evident to the eye. The inset shows the horizontal particle current for $\rho = 0.35$ (circles), 0.20 (crosses), and 0.10 (squares).

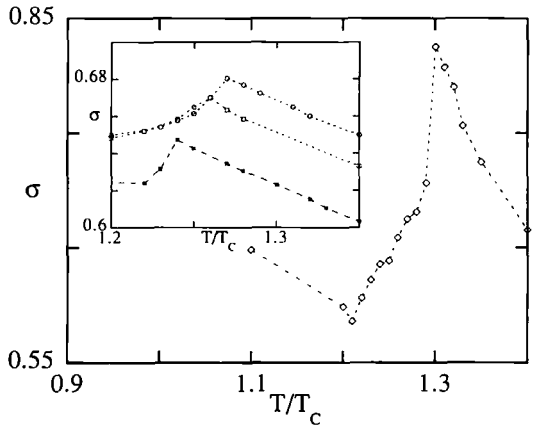

Fig. 8. The short-range order parameter, as defined in the text, for the infinite lattice. The existence of a peak at T_∞^* seems to exclude the possibility that $\beta = 1/2$.[22] The inset shows data for finite L: the peak locating the transition temperature increases and shifts toward larger temperatures as L is increased.

Following a previous suggestion,[22] we have computed the quantity $\sigma = [(1/4)(2-e)^2 - m^2]/e^2$, which plays the role of a short-range order parameter. The fact that σ exhibits a well-defined peak at $T_\infty^*(\rho = 1/2)$ in Fig. 8 indicates[22] that the critical behavior of the system cannot be of the Landau type, e.g., $\beta \neq 1/2$. We have also found very useful the parameter σ (which exhibits simple scaling behavior) in making precise our values for the transition temperatures for the finite lattice and thus for $|\Lambda| \to \infty$.

3.2. Correlations

An interesting question is the behavior of spatial correlations. We have monitored the spin–spin correlation function at each plane, $i = 1, 2$, namely,

$$G_i(\mathbf{r}) = |\Lambda|^{-1} \left\langle 4 \sum_{\mathbf{r}'} (\sigma_{\mathbf{r}'} - \rho_i)(\sigma_{\mathbf{r}+\mathbf{r}'} - \rho_i) \right\rangle \tag{3.5}$$

where $\langle \cdot \rangle$ denotes the MC average over configurations. We define $G(\mathbf{r})$ (unless otherwise indicated) as either the case of (3.5) which corresponds to the plane with segregation or else $G(\mathbf{r}) = 1/2[G_1(\mathbf{r}) + G_2(\mathbf{r})]$ when segregation occurs in both planes. Moreover, it is advisable to study separately the two main directions; therefore, we have computed the horizontal spin–spin correlation function, say $G_h(x, 0)$, where x refers to the direction of the field [for simplicity, we denote this function as $G_h(r)$,

with $r \equiv x$, hereafter], and the vertical component, denoted $G_v(0, y)$ [or simply $G_v(r)$, $r \equiv y$]. The structure function is defined as

$$S(\mathbf{k}) = (2|\Lambda|)^{-1} \left\langle \sum_{\mathbf{r}} |2e^{i\mathbf{k}\cdot\mathbf{r}}(\sigma_{\mathbf{r}} - \rho)|^2 \right\rangle \tag{3.6}$$

where $\mathbf{k} = (k_x, k_y, k_z)$, where k_x and k_y describe the first Brillouin zone and $k_z = 1$ or 0 refers to the two planes.

Unlike typical studies of both the ordinary lattice gas and the DLG, the structure function (3.6) remains rather stable in practice during the *stationary regime* (see the end of Section 2) in our experiments. For $\rho = 1/2$, (3.6) is observed to exhibit a pronounced peak at $\mathbf{k} = (0, 0, 1)$ for $T < 0.95 T_C$, which corresponds to having phase segregation in only one of the planes, while the peak moves toward $\mathbf{k} = (1, 0, 0)$ as T is increased, which corresponds to the formation of two strips. The situation is similar for $\rho < 1/2$. This phase transition as well as the one at higher temperature described above is nicely confirmed by looking at the spin–spin correlation between planes, which provides also a simple method to estimate accurately transition temperatures for this system, as illustrated in Fig. 9.

The components of $S(\mathbf{k})$ for appropriate values of $\mathbf{k}$ may also characterize the striped geometry. For instance, one may study the parameter[9]

$$n = [(m_h^{(\sin)})^2 + (m_h^{(\cos)})^2 + (m_v^{(\sin)})^2 + (m_v^{(\cos)})^2]^{1/2} \tag{3.7a}$$

where

$$m_h^{(\sin)} = \frac{\pi}{2L_h L_v} \sum_{x=1}^{L_h} \sum_{y=1}^{L_v} \sigma_{x,y} \sin\left(\frac{2\pi}{L_h} x\right) \tag{3.7b}$$

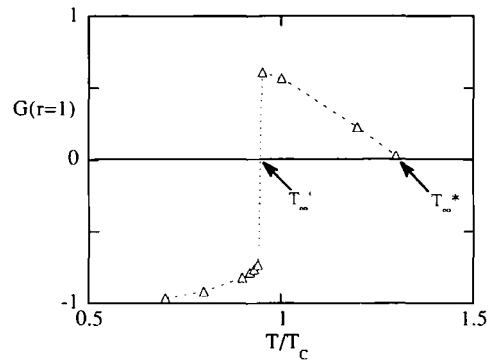

Fig. 9. The correlation function between planes (for $r = 1$), as a function of temperature, for $\rho = 1/2$ and $L = 70$, confirming that $T_\infty^* \approx 1.3 T_C$.

etc.; here, $L_h L_v = |\lambda| = 1/2\,|A|$; generally, we considered the case $L_h = L_v = L$. We checked that the critical behavior of $n(T)$ for $\rho = 1/2$ is consistent with the exponent $\beta \approx 1/4$ found above for $m(T)$, $\Delta\rho(T)$, and $\delta\rho(T)$ (cf. Fig. 6 for some evidence), but no further interesting qualitative facts ensued from our study of (3.7), which turns out to be less convenient for computational purposes than the other parameters.

A specific question here is the nature of correlations for $\rho = 1/2$ and $T < T'_\infty$, where we have observed both that the (nonequilibrium) liquid and gas phases have a density very close to the equilibrium case, $\rho_\infty(T) \approx \rho_0(T)$, and that no interface exists (given that the liquid then fills completely one of the planes). The study of $G(\mathbf{r})$ gives further support to the result $\rho_\infty(T) \neq \rho_0(T)$ which is suggested by the raw data, e.g., in Table II; cf. Fig. 10. The latter indicates that $G_h(r)$ differs essentially depending on whether $E = 0$ or $E \neq 0$, and that $G_h(r) \neq G_v(r)$ for $E = \infty$ as long as r remains small enough, while the two functions become equal for $r > 3$. Figure 11, on the other hand, illustrates the case $\rho < 1/2$ and $T < T'_\infty(\rho)$, where one still has that $\rho_\infty(T) \approx \rho_0(T)$ (cf. Fig. 2), but there is an interface, unlike for Fig. 10. Figure 11 reflects the differences in $G_v(r)$ between the equilibrium and nonequilibrium cases for large r due to the existence of a special interface. For qualitative purposes, in Fig. 12 we compare $G_h(r)$ and $G_v(r)$ for $\rho = 1/2$ at different values of the temperature which correspond to the three kinds of steady states the system may exhibit.

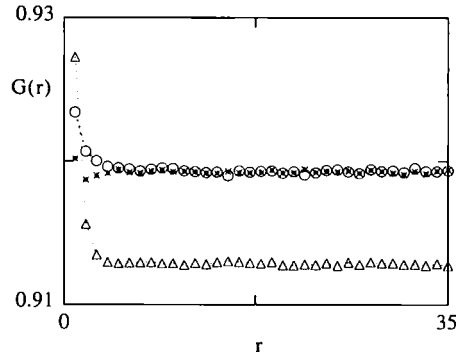

Fig. 10. The correlation function for $\rho = 1/2$, $T = 0.8T_C$ ($< T'_\infty$), and $L = 70$. The circles and the triangles correspond to horizontal correlations for $E = \infty$ (nonequilibrium) and $E = 0$ (equilibrium), respectively; the asterisks represent vertical nonequilibrium correlations. In accordance with Table II, the two asymptotic values are $\rho_\infty^2 = (0.959)^2$ and $\rho_0^2 = (0.955)^2$, respectively, as expected.

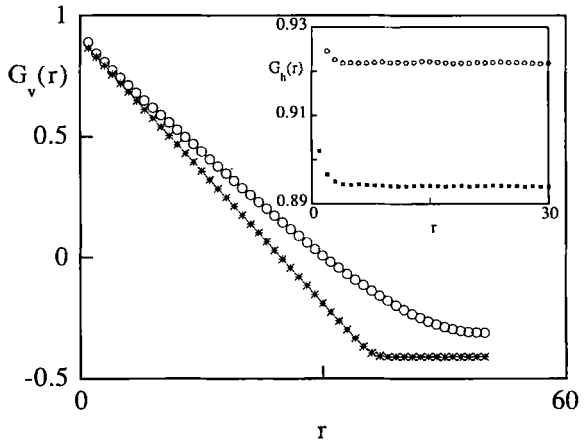

Fig. 11. The asterisks represent the function $G_v(r)$ for $\rho < 1/2$ and $T < T'_\infty(\rho)$ in the plane which contains the striped liquid; the circles represent the corresponding result at equilibrium ($E = 0$). The inset is for the horizontal correlations within the gas plane for $E = 0$ (circles) and $E = \infty$ (asterisks).

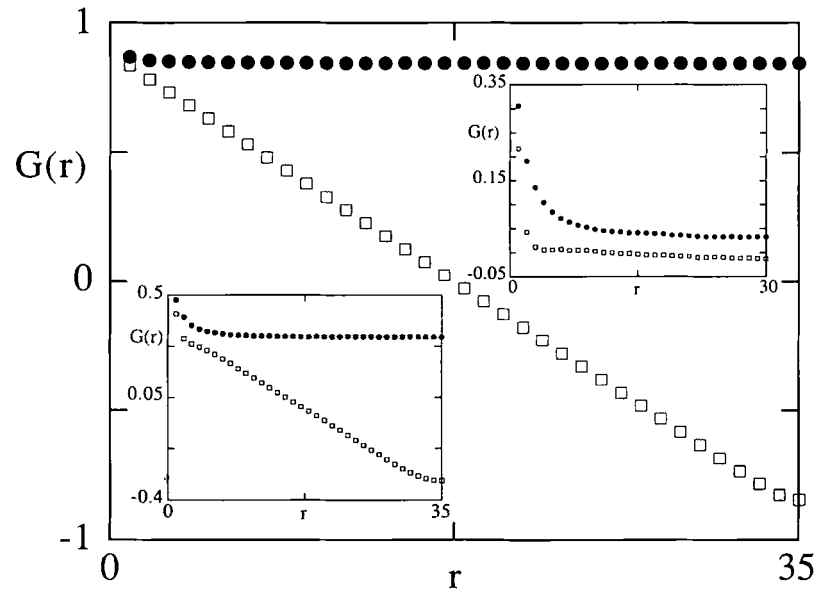

Fig. 12. The nonequilibrium correlation functions $G_h(r)$ (solid circles) and $G_v(r)$ (squares) for $L = 70$, $\rho = 1/2$, and $T/T_C = 0.80$ (main graph), 1.21 (lower inset), and 1.32 (upper inset).

As a paradigm of a nonequilibrium lattice gas with conserved density, the 2d DLG exhibits slow, power-law decay of $G(\mathbf{r})$ with $\mathbf{r}$ at high temperature (instead of the exponential relaxation that characterizes the equilibrium systems except at criticality).[23] The question is whether this occurs for A_∞. The latter exhibits anisotropic clustering in the one-phase region, as described above, but this is not necessarily the hallmark of slow

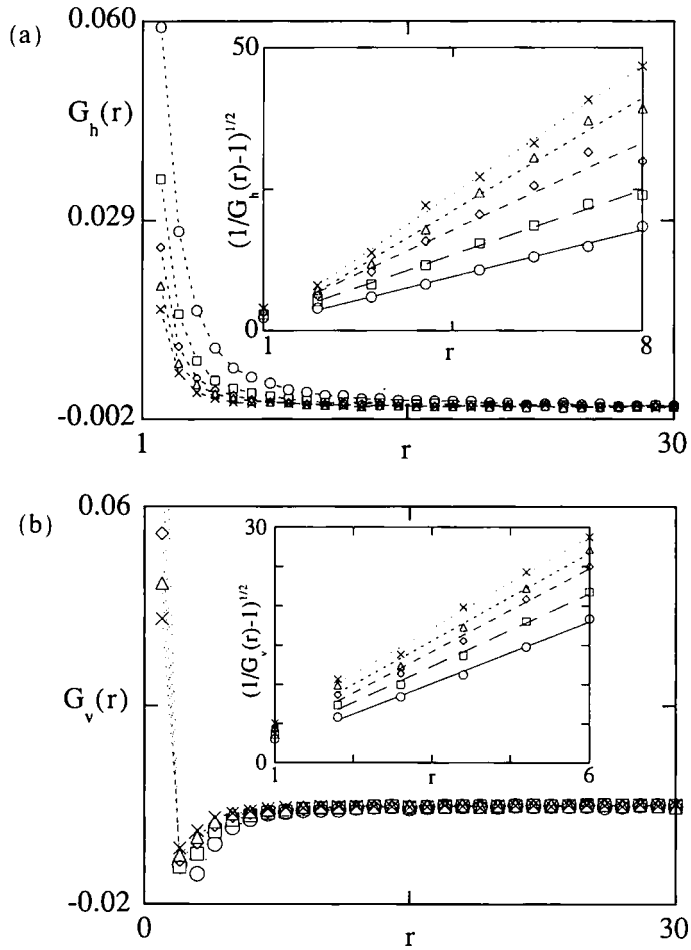

Fig. 13. (a) The horizontal correlation function for different values of temperature, $T/T_C = 2.5$ (circles), 3.5 (squares), 4.5 (rhomboids), 5.5 (triangles), and 6.5 (crosses). The inset is a linear fit to the same data, as indicated, to obtain the correlation length, i.e., the slope of the lines corresponds to $1/\xi_h(T)$. (b) The same, for the vertical correlation function; the inset refers to the absolute value $|G_v(r)|$.

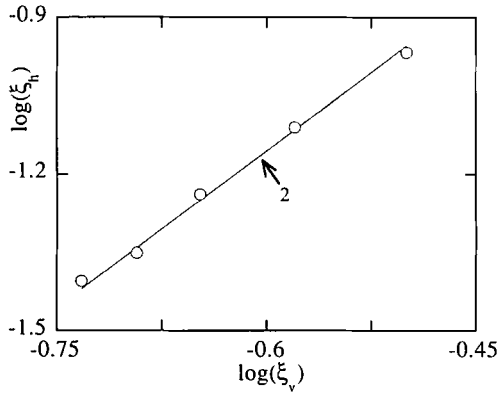

Fig. 14. The relation between the two possible correlation lengths, each obtained as indicated by the insets in Fig. 13, to reveal that data are consistent with $\nu_h \approx 2\nu_v$.

decay of correlations. Furthermore, one may argue that correlations should perhaps not decay here as slowly as for λ_∞ given that particles can hop to another plane in A_∞ (e.g., the structure function is more easily stabilized due to this effect). The latter expectation is not confirmed, however, in a detailed study of $2 \times 140 \times 140$ lattices for temperatures $1.4 < T/T_C < 6.5$, which reveals a behavior similar to the one for the 2d DLG at high T; cf. Fig. 13. That is, a log–log plot of both $G_h(r)$ and $G_v(r)$ produces straight lines of slope -2 for any $2 \leqslant r \leqslant 20$ (the noise dominates for $r > 20$, but one may guess the same behavior from the data) for any $T \geqslant 2.5T_C$; this supports the expected result $G(x, y) = (ax^2 - by^2)(x^2 + y^2)^{-2}$.

One may estimate the correlation length from the phenomenological fit $G_{h,v}(r) \sim [1 + (r/\xi_{h,v})^2]^{-1}$, which is confirmed by the data for *large enough* r. The values of ξ_h and ξ_v obtained in this way (cf. the inset in Fig. 13) have critical behavior at $T^*_\infty(\rho = 1/2)$ which may be characterized by the exponents ν_h and ν_v, respectively. As illustrated in Fig. 14, the data provide some evidence that $\nu_h \approx 2\nu_v$. Moreover, we have estimated that $\nu_h = 0.7 \pm 0.2$ and $\nu_v = 0.4 \pm 0.2$; this is to be compared to the field-theoretic values $\nu_h = 1 + \varepsilon/6$ and $\nu_v = 1/2$ for $\varepsilon = 5 - d$[10]; cf. Section 4, however.

We have also compared the high-T (gas) phase and the gas phase that coexists with liquid at low enough T (Fig. 15). Figure 15a reveals that vertical correlations are very similar to each other, while horizontal ones differ, except perhaps for small r. Figure 15b indicates that there is no more evidence of an exponential behavior for low T than for high T, and that the power of -2 is not supported at low $-T$, while it is a reasonable description of the data at high T.

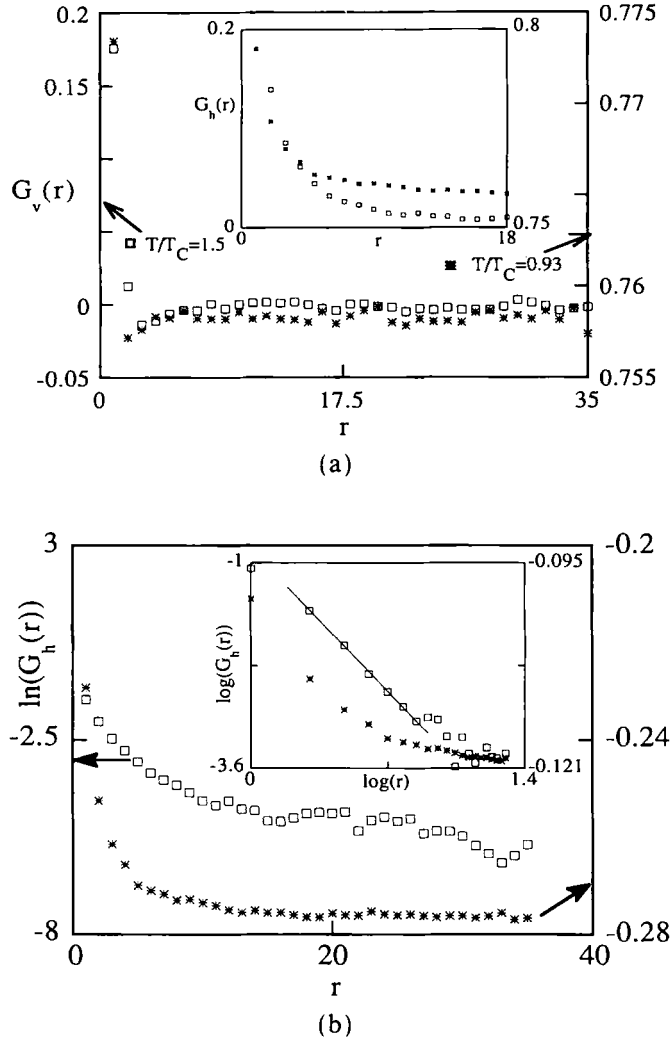

Fig. 15. A comparison of the high-T (squares) and low-T (asterisks) gas phases; the latter coexists with liquid. (A double axis representation is used to enhance the comparison.) (a) The vertical (main graph) and horizontal (inset) correlations for $T/T_C = 1.5$ and 0.93, as indicated. (b) The horizontal correlation for $T/T_C = 2$ (squares) and 0.93 (asterisks). The main graph is ln G versus r, looking for exponential behavior. The inset is a log–log plot looking for power-law behavior; the solid line has slope -2.

3.3. Scaling of Data with Size

Several sorts of finite-size scaling analysis have been proposed for anisotropic systems[7, 9, 10, 24, 25] that are not always compatible with each other in spite of their phenomenological character. The simplest (i.e., avoiding any elaborate assumption) scaling-with-size ideas have been used by us to obtain some of the behavior for the infinite system (as reported above) from that for finite $|\Lambda|$. As a further test of critical behavior, we applied the approach in refs. 9 and 24 to a series of independent data. Let a (rectangular) system with linear dimensions L_h and L_v be a subsystem of the infinite system with $\rho = 1/2$ at critical temperature T^*_∞. Our *infinite system* consists of a $2 \times 128 \times 128$ lattice; 25 subsystems of different sizes, $L_h \times L_v = 2^i \times 2^j$ at each plane, with $i, j = 2, 3, 4, 5, 6$, have been considered. The system evolved for 3×10^5 MC steps (per site) and the *stationary regime lasted for* 5×10^5 MC steps more. We consider a local order parameter, say $|\Psi_l|$, defined as the mean absolute value of the magnetization within subsystem l averaged over configurations (this is a fluctuation allowed for by particle diffusion between subsystems).

Let us denote by χ the corresponding susceptibility. It is assumed from the start that $\nu_h \neq \nu_v$; then, the main predictions are that

$$|\Psi| \propto L_v^{-\beta/\nu_v} \quad \text{for} \quad L_h \ll L_v^{\nu_h/\nu_v} \tag{3.8a}$$

$$|\Psi| \propto L_h^{-\beta/\nu_h} \quad \text{for} \quad L_h \gg L_v^{\nu_h/\nu_v} \tag{3.8b}$$

and that

$$\chi \propto L_h L_v^{\gamma/\nu_v - \nu_h/\nu_v} \quad \text{for} \quad L_h \ll L_v^{\nu_h/\nu_v} \tag{3.9a}$$

$$\chi \propto L_v L_h^{\gamma/\nu_h - \nu_v/\nu_h} \quad \text{for} \quad L_h \gg L_v^{\nu_h/\nu_v} \tag{3.9b}$$

The quantities χ and $|\Psi|$ are represented in Fig. 16 as a function of L_h and L_v. The assumption (3.8) is apparently not supported by the data (for the system sizes that we have investigated), while there seems to be some weak support for (3.9). Thus, we do not give much credit to the numerical estimates we have obtained in this way, but it is worth mentioning that any manipulation of the data in the main graph of Fig. 16 (and, to some extent, also the one in the inset) on the assumption (3.9) [and (3.8)] gives support to our conclusion above that $\beta \approx 1/4$. [It should perhaps be remarked that the amount of data that we have specifically generated to analyze (3.8) and (3.9) is small compared to that to which we refer in the rest of our study, but is comparable to previous studies of rectangular lattices. The same is true for a series of nonsystematic runs using

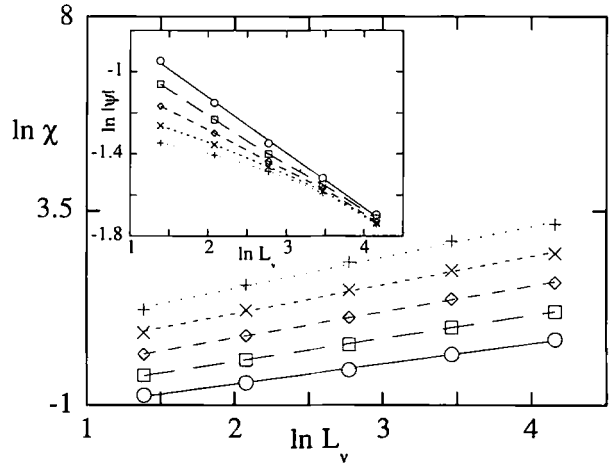

Fig. 16. Log–log plot of the ordering susceptibility for rectangular, $L_h \times L_v$, subsystems, as a function of L_v for several values of the other linear dimension: $L_h = 4$ (circles), 8 (squares), 16 (rhomboids), 32 (×), and 64 (+). The inset shows the same for the magnetization order parameter $|\Psi|$.

rectangular lattices we have performed in which (e.g.) some of the questions raised in Figs. 10–15 were investigated. We thus came to believe that a rectangular geometry is probably not essential to generate good data, while it results in a much more involved computational procedure. The same may perhaps be suspected from the behavior of correlations in Figs. 10, 11, 13, and 14, for instance.]

The attitude expressed by the referees during the editorial process has persuaded us to put some further effort into this problem. The question is to understand the classical behavior (e.g., $\beta = 1/2$) that was apparently found for λ_∞ in one of the previous numerical experiments.[10] We have studied the case of one plane with rectangular, $L_h \times L_v$ geometries, looking for the anisotropic scaling behavior,

$$M = L_h^{-1/3} \tilde{M}(t L_h^{2/3}), \qquad t \equiv |T_\infty^* - T|/T_\infty^* \tag{3.10}$$

which is implied by the proposed continuum version of the DLG. The same quantities and even sizes have precisely been considered, while our MC runs have typically lasted four times or more as long (i.e., up to 9×10^6 MC steps) as the ones in ref. 10. As a first conclusion, we have thus confirmed the explicit finding in ref. 14 that the consideration of a second, uncoupled

lattice is convenient to study numerically phase coexistence in systems with a conserved density. In particular, we have not been able to obtain for one plane data of a quality similar to that above for Λ_∞. A second general conclusion is that the order parameter exhibits a weak dependence (if at all) on the proposed anisotropy parameter $s \equiv L_h^{1/3} L_v^{-1}$. Therefore, it is difficult to come to a definitive conclusion on this specific problem based only on numerical data. However, we have obtained the clear evidence depicted in Fig. 17 (see the figure caption). The departure from scaling behavior is even more dramatic (not shown) if one uses instead $T_\infty^* = 1.38$, which is rather suggested to us by the raw data, while one observes (see the inset in Fig. 17) a tendency to collapsing of data as β is decreased. It is doubtful, however, whether one should ascribe any significance at all to the latter fact. (The inset in Fig. 17 reveals a systematic—albeit small—departure of the data in ref. 10 from the present case, which might be related to the relatively short duration of the runs in the former case.)

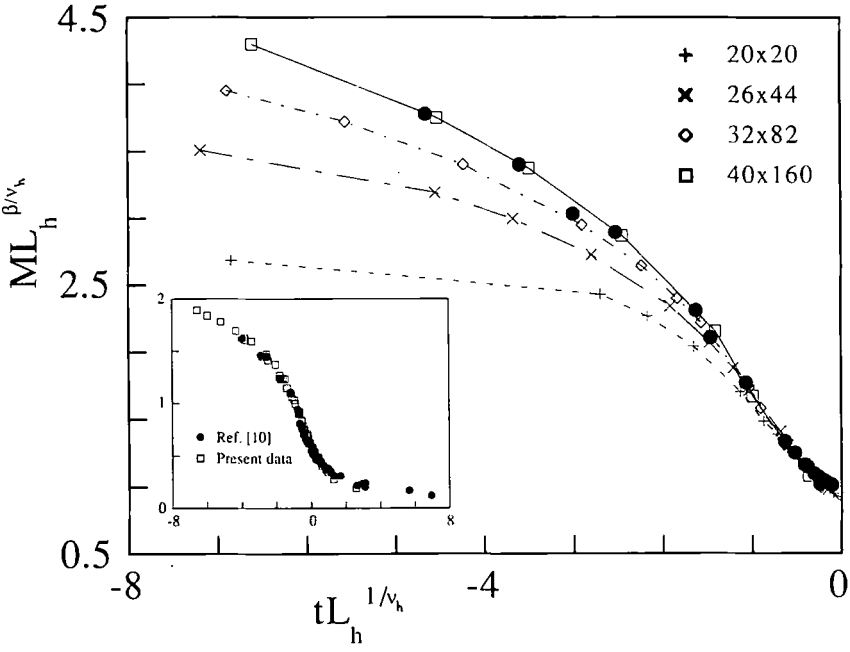

Fig. 17. A plot of the order parameter, as suggested in ref. 10, for λ_∞ with $\beta = 1/2$, $\nu_h = 3/2$, and $T_\infty^* = 1.418$. Different symbols correspond to different sizes as indicated; the solid circles correspond to data reported previously.[10] The inset shows the same, but for $\beta = 1/4$.

4. A BRIEF DISCUSSION

We have related to each other the nonequilibrium system Λ_∞, the ordinary two-dimensional DLG, λ_∞, and the ordinary lattice gas, λ_0; a simple relation exists between the latter and the lattice gas in two planes, Λ_0.[14] The nature of both short- and long-range correlations and the existence for some values of T and ρ of a nonequilibrium anisotropic interface whose length is proportional to one of the system linear dimensions make Λ_∞ essentially different from its equilibrium counterpart Λ_0. There seems to be a relation between Λ_∞ and λ_∞, however, that, in particular, makes the study of an apparently artificial model relevant for nonequilibrium theory; Λ_∞ has an intrinsic interest and perhaps some practical relevance as well, as indicated in Section 1. [The relation between Λ_∞ and λ_∞ has been studied analytically within a mean-field approximation (also to be published).]

The MC study of Λ_∞ turns out to be more rewarding than that of λ_∞ (and even more than that of the familiar λ_0). In any case, our study should be considered as quantitative only for $\rho = 1/2$, which corresponds to the unique critical point. We have determined some properties of the latter, e.g., the critical temperature is 30% above the Onsager result, and the critical exponent for the order parameter is $\beta \approx 1/4$ (probably $\beta \approx 0.27$). The field-theoretic value $\beta = 1/2$ for a related continuum model may be discarded with as much confidence as the equilibrium case $\beta = 1/8$. We cannot make assertions with such conviction about the other exponents. There is some weak evidence that $\alpha > 0$ and, assuming that horizontal (the field direction) and vertical correlations should diverge differently (as for field-theoretic models), we obtain that $\nu_h \approx 2\nu_v$ for the corresponding exponents. Much more data would be needed to conclude more definitely about the last two facts, which to our knowledge, have not been observed before. We remark, however, that further numerical effort requires a better understanding of scaling behavior for the present problem. In fact, no support has been obtained here for the sort of scaling in refs. 10 and 24. In particular, we have measured $\beta \approx 1/4$ for both cases $L_h = L_v$ and $L_h \neq L_v$, and it is our belief that one should not rule out completely for the moment the possibility that *effective* ν_h and ν_v tend to each other as one approaches the critical point. Anyhow, the fact that the size more than the shape of the system matters for critical behavior is suggested by our study. On the other hand, it may be mentioned that, from a purely computational point of view, the situation when one tries to estimate critical indexes is not worse here due anisotropies than for the equilibrium case $E = 0$, e.g., critical slowing down seems a more important effect than slow spatial decay of correlations. For practical purposes, it is also noticeable that the facts that (3.3) exhibits relatively large finite-size effects at high temperature and misses

some important information about the spatial distribution of domains[9, 10] do not seem to diminish its utility in the present problem; e.g., (3.3) is computationally convenient, and we have checked that it has similar qualitative and critical behavior as (2.6), (3.2), and (3.7).

Our study of Λ_∞ for $\rho < 1/2$ should be viewed as qualitative or, at most, semiquantitative, i.e., our computation of transition temperatures is hampered by important metastability for $\rho \ll 1/2$, and we never estimated the size dependence for off-critical densities. Moreover, a peculiar finite-size effect that has been revealed in the study of Λ[14] is present here. That is, for a finite system the fraction of the liquid phase for given ρ is smaller for Λ_∞ than for λ_∞; therefore, the coexistence line for the former occurs before that for the latter if one increases T for given ρ. As in equilibrium,[14] this effect is expected to be noticeable only for small enough T and ρ, e.g., for $\rho \leqslant 0.2$, but probably not for $\rho \geqslant 0.3$. In any case, we have studied in detail the nature of the phases for both $\rho = 1/2$ and $\rho < 1/2$, including comparisons with the equilibrium case. It is also interesting to see the apparently different nature of correlations for the gas phase at low and high temperature.

ACKNOWLEDGMENTS

We acknowledge useful discussions with Dr. P. L. Garrido and some leading comments by Dr. J. L. Lebowitz at an early stage of this work. The financial support of the Dirección General de Investigación Científica y Técnica (PB91-0709) and Plan Andaluz de Investigación (Junta de Andalucía) of Spain is acknowledged.

REFERENCES

1. P. L. Garrido, J. Marro, and R. Dickman, *Ann. Phys.* (NY) **199**:366 (1990), and references therein.
2. H. Spohn, *Large Scale Dynamics of Interacting Particles* (Springer-Verlag, Berlin, 1991), and references therein.
3. J. Marro, P. L. Garrido, and J. L. Vallés, *Phase Transitions* **29**:129 (1991), and references therein.
4. S. Katz, J. L. Lebowitz, and H. Spohn, *J. Stat. Phys.* **34**:497 (1984).
5. J. Marro, J. L. Lebowitz, H. Spohn, and M. H. Kalos, *J. Stat. Phys.* **38**:725 (1985).
6. J. L. Vallés and J. Marro, *J. Stat. Phys.* **43**:441 (1986).
7. J. L. Vallés and J. Marro, *J. Stat. Phys.* **49**:89 (1987).
8. J. Marro and J. L. Vallés, *J. Stat. Phys.* **49**:121 (1987).
9. J. S. Wang, K. Binder, and J. L. Lebowitz, *J. Stat. Phys.* **56**:783 (1989).
10. K. Leung, *Phys. Rev. Lett.* **66**:453 (1991); see also K. Leung, *Int. J. Mod. Phys. C* **3**:367 (1992), and references therein.

11. K. Gawadzki and A. Kupiainen, *Nucl. Phys. B* **269**:45 (1986).
12. H. K. Janssen and B. Schmittmann, *Z. Phys. B* **64**:503 (1986).
13. K. Leung and J. L. Cardy, *J. Stat. Phys.* **44**:567 (1986).
14. A. Achahbar, P. L. Garrido, and J. Marro, to be published.
15. C. N. Yang and T. D. Lee, *Phys. Rev.* **87**:404, 410 (1952).
16. Z. Cheng, P. L. Garrido, J. L. Lebowitz, and J. L. Vallés, *Europhys. Lett.* **14**:507 (1991).
17. J. L. Vallés, *J. Phys. I* (Paris) **2**:1361 (1992).
18. F. J. Alexander, I. Edrei, P. L. Garrido, and J. L. Lebowitz, *J. Stat. Phys.* **68**:497 (1992).
19. E. L. Praestgaard, H. Larsen, and R. K. P. Zia, *Europhys. Lett.* **25**:447 (1994).
20. B. Schmittmann and R. K. P. Zia, *Phys. Rev. Lett.* **66**:357 (1991).
21. C. K. Chan and L. Lin, *Europhys. Lett.* **11**:13 (1990).
22. J. Marro, P. L. Garrido, A. Labarta, and R. Toral, *J. Phys.: Condensed Matter* **1**:8147 (1989).
23. P. L. Garrido, J. L. Lebowitz, C. Maes, and H. Spohn, *Phys. Rev. A* **42**:1954 (1990).
24. K. Binder and J. S. Wang, *J. Stat. Phys.* **55**:87 (1989).
25. S. M. Bhattacharjee and J. F. Nagle, *Phys. Rev. A* **31**:3199 (1985).